AADE-19-NTCE-097

High-Frequency Torsional Oscillation Study with a Motor-Assist Push-the-Bit Rotary-Steerable System and Multiple High-Frequency (800Hz) Drilling Dynamics Recorders in North America Land

Junichi Sugiura and Steve Jones, Sanvean Technologies

Abstract

Motor-assist rotary-steerable system (RSS) bottom-hole assemblies (BHA's) are often used for increasing drilling performance in horizontal sections of shale oil and gas drilling in the United States. Downhole drilling dysfunctions, such as high-frequency torsional oscillation (HFTO), are commonly observed especially when the BHA's are pushed to the limit for maximum drilling performance. To understand the propagation and characteristics of the harmful HFTO, high-frequency continuous recording compact drilling dynamics sensors were embedded into the bit box and outer housing of the RSS, and drive mandrel and top sub of the motor. Three-axis, high-dynamic-range (+/-200g) accelerometers were sampled at 800Hz and continuously recorded in memory in multiple positions of the motor-assist RSS BHA. To compare various field test results, sensor offset distances (from the tool center) on each position of the BHA were given to associate angular acceleration magnitudes when the BHA was exposed to HFTO.

The motor-assist RSS BHA was simulated with an analytical model and finite-element analysis model to enhance the understanding of self-perpetuating HFTO, which occurs with typical motor-assist RSS BHA's. Simulation results revealed that non-torsional natural frequencies occur at lower frequencies and, at torsional natural frequencies, HFTO magnitude is highest near the bit and near the surface of the structure.

Introduction

In North American shale drilling applications with a motor-assist RSS, medium-to-severe downhole drilling dysfunctions, such as torsional vibrations, are often encountered. There are two major types of self-excited torsional oscillations: low-frequency torsional oscillation (LFTO) and high-frequency torsional oscillation (HFTO) [1-3]. A well-known type of the LFTO is stick-slip in which a drill bit and/or drillstring change their rotation speed periodically, alternating "stick" and "slip" phases [4-8]. The bit and/or drillstring could completely stop rotating in the "stick" phase of the severe stick-slip conditions. The oscillation frequency of stick-slip (f_n) often corresponds to the fundamental mode ($n = 1$) of torsional resonance of the entire drillstring, for example, from the top drive to the drill bit, as defined by **Eq. 1**:

$$f_{n(fixed-free)} = \frac{(2n-1)}{4L}\sqrt{\frac{G}{\rho}} \quad \text{..... Eq. 1}$$

where G = shear modulus of the drillstring, ρ = density of the steel, L = drillstring length (e.g. *9000ft*), and $n = 1, 2, 3, \ldots$

As can be seen, the boundary condition of the surface side (e.g. the top drive) is "fixed" and the boundary condition of the drill-bit side is "free". The fundamental mode (first-order mode) oscillation frequency is calculated with $n = 1$. Some researchers conducted the study on the higher-mode stick-slip frequencies [9,10]. For a long time, it was believed that mud motors isolate or "de-couple" stick-slip to the bit, but recent studies with downhole sensors reported that the LFTO and stick-slip (from the drillstring) could travel to the bit, which affect the drilling efficiency and the bit/BHA life [2,11,12].

Surface systems and/or standard measurement-while-drilling (MWD) tools are used to detect the stick-slip phenomena in real-time and/or memory-recording modes [13,14]. Many researchers have studied stick-slip in the past several decades as the phenomena are relatively easily captured [3-8,15,16].

High-frequency torsional oscillation (HFTO) is the other type of self-excited torsional oscillations similar to stick-slip, but the HFTO frequencies are typically observed above 50Hz and sometimes, more than 560Hz [1,11,12,17-23]. HFTO have only been reported in relatively recent years because of advances in measurements and placement of sensors. Historically HFTO could not be detected from downhole sensors because 1) the standard MWD tools cannot measure and record HFTO due to its high frequency, and 2) HFTO originating from the drill bit and lower part of the BHA is attenuated very quickly and often does not travel to the surface. This is especially true with a steerable motor BHA and motor-assist RSS BHA, because the HFTO energy is resonated to the structure below the motor and "trapped" below the motor [11,12,18,19].

HFTO is thought to originate from very high-frequency shocks generated by the interaction between the Polycrystalline Diamond Compact (PDC) cutters and formation, which is resonated with the lower BHA structure [17-19]. It is known that HFTO is more likely to occur while drilling hard and dense

formations [1,18,19]. A simple model based on Eq. 1 can provide torsional natural frequencies for the lower part of the BHA [12,21]. Finite-element analysis (FEA), harmonic dynamic simulation, and transient dynamics simulation are used for more accurate modeling of HFTO frequencies and mode shapes. [11,12,18-23].

The extremely harmful nature of HFTO can cause accelerated fatigue failure due to high-frequency, high-amplitude torsional strain in the BHA, shock-sensitive electronics-component failure, and collar cracking, which are reported, for example, by Lines et al. (2013), Oueslati et al. (2013), and Zhang et al. (2017) as shown in **Fig. 1** [11].

Fig. 1: 45° collar cracking (third-party tool) due to severe HFTO (excerpted from SPE-187173)

HFTO and its damaging nature were undetected and unknown until recently (less than 10 years) because the measurement of HFTO requires a compact high-frequency drilling dynamics recorder to be deployed close to the drill bit, such as in the drill bit, bit box, motor lower mandrel or carrier sub behind the bit. The carrier sub option is typically not preferred in the case of a conventional steerable motor or RSS since this will interfere with the directional response and stability of the BHA.

This paper presents the HFTO observations with 3 different motor-assist RSS BHA's used to drill in West Texas. Embedded compact high-frequency drilling dynamics recorders were used to acquire actual downhole data at the points of interest. Case studies from all BHA's show the predicted HFTO frequencies and their mode shapes, based on simulations. The actual downhole field-measured dominant HFTO frequencies are displayed in spectrograms.

RSS with Embedded Sensors

A digitally-controlled rotary-steerable system (RSS), extensively embedded with electronics, solid-state sensors and an electrically controlled mud valve, has been developed specifically for drilling vertical, nudge, tangent and lateral well profiles from pads in North America [26]. This push-the-bit RSS includes a slow-rotating steering housing with four mud activated pads to apply side force at the bit as shown in **Fig. 2**. Controlled pad activation is achieved using a novel mud valve driven by a low-power electric motor and gearing system.

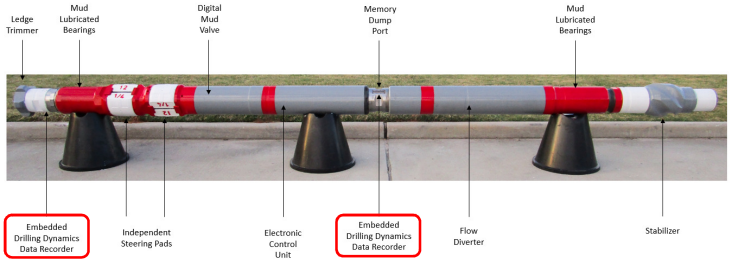

Fig. 2: Side view of 9 5/8-in RSS highlighting key components and features (excerpted from SPE-189705)

The electronics measurement and control system are mounted in the slow-rotating steering housing and includes 3-axis inclinometers, 3-axis magnetometers, 3-axis shock sensors, 3-axis gyros, and temperature sensors. Additionally, compact drilling dynamics sensors are placed at the bit box to gather at-bit data to evaluate bit-rock dynamic interaction [12].

Mud Motor with Embedded Sensors

Drilling dynamics sensors are embedded into the bit box and top sub of the latest-generation mud motor as shown in **Fig. 3** [27,28].

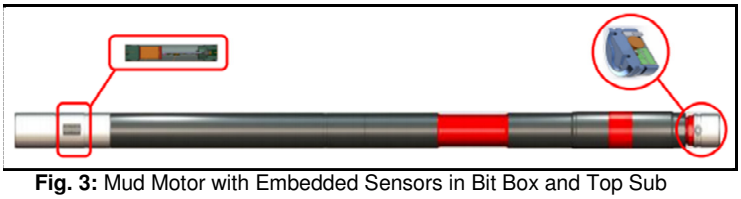

Fig. 3: Mud Motor with Embedded Sensors in Bit Box and Top Sub (excerpted from AADE-17-NTCE-077)

The sensors are installed into existing mud motors without additional length and/or additional connections and without compromising the mechanical integrity of the motor.

Downhole Measurements

The embedded high-frequency (HF) sensors are designed to be compact enough to fit into the RSS bit box, existing motor mandrel bit box and top sub without having to build new assets. The design allows for modification of new and existing tools to accept the sensors.

All vertical, nudge, tangent and lateral motor-assist RSS BHAs are embedded with HF (800Hz) compact drilling dynamics sensors to record BHA dynamics at critical points throughout the BHA. The embedded sensors are installed in the RSS bit box, the RSS slow-rotating housing, the mud motor drive mandrel and the mud motor top sub as shown in **Fig. 4**. The configuration and deployment of the embedded sensors are

similar to the fully mechanical RSS described in Jones et al. [29]. The memory-only sensors provide data for post-run evaluation which is especially useful when drilling "at-the-limit". Recorded drilling dynamics data allows dynamic performance to be evaluated, as well as mapping of optimal formation-related drilling parameters for future wells in the area.

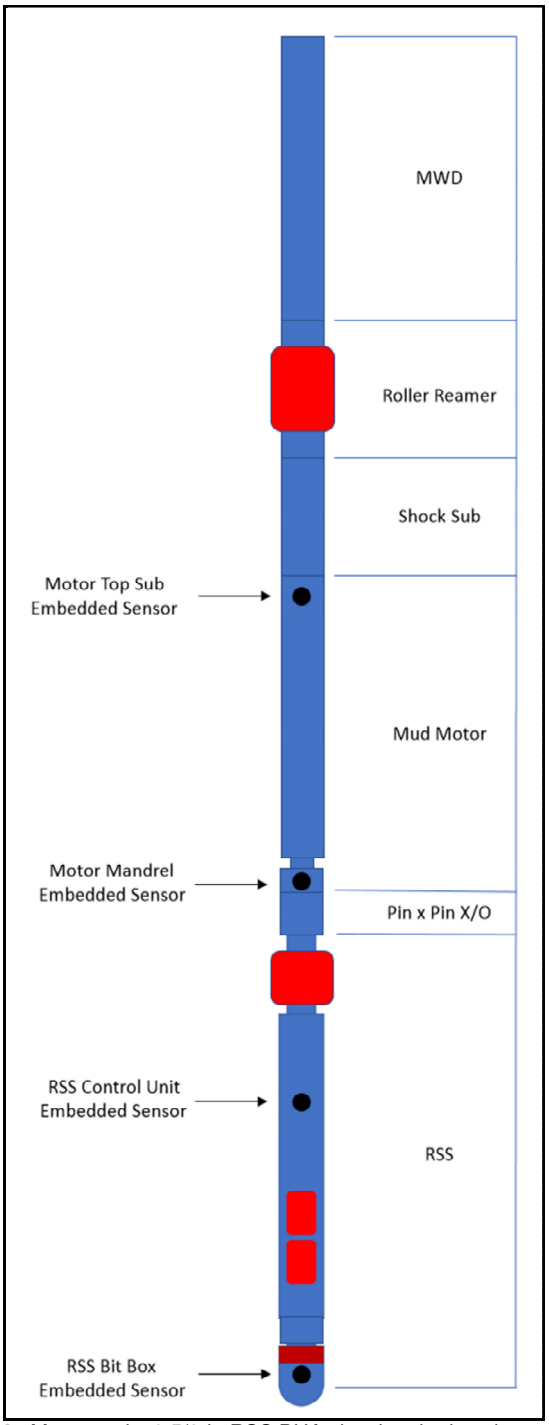

Fig. 4: Motor-assist 9 5/8-in RSS BHA showing the locations of the embedded drilling dynamics data recorders (excerpted from SPE-189705)

Table 1 shows the specification of the newly developed compact drilling dynamics sensors used in this study. A motor-assist RSS BHA with multiple high-frequency (800Hz) drilling dynamics sensors allows the in-depth analysis of the drilling dysfunctions in very challenging drilling conditions.

Table 1: Two versions of the compact HF drilling dynamics sensors

	Extended-Memory Version (Second Generation)	Extended-Battery Version (Third Generation)
3-axis high-g accelerometers (-200g to 200g)	Continuous Recording (800-1600Hz)	Continuous Recording (800-1600Hz)
3-axis low-g accelerometers (-16g to 16g)	Burst (25-100Hz)	Burst (25-100Hz)
Gyro (-333rpm to 333rpm)	Burst/Continuous (20-100Hz)	Burst/Continuous (20-100Hz)
3-axis magnetometers (-40 gauss to +40 gauss)	N/A	Burst (20-100Hz)
Temperature Sensor	-40°C to 150°C (160°C version available)	-40°C to 150°C (160°C version available)
Pressure Rating	15000 PSI	15000 PSI
Length	3.8 in.	5.8 in.
Diameter	¾ in.	¾ in.
Battery Life	Continuous Logging Up to 51 hours (at 1600Hz) Up to 102 hours (at 800Hz)	Continuous Logging Up to 136 hours (at 1600Hz) Up to 272 hours (at 800Hz)

Fig. 5 shows the sensor package housed within a ¾-in diameter and 3.8-in long pressure barrel. The "standard" and "extended-battery" versions are available in this package (both with the ¾-in diameter). The standard version can record three-axis accelerations continuously at 800Hz for 102 hours. The "extended-battery-life" version can perform the 800Hz continuous logging for 272 hours.

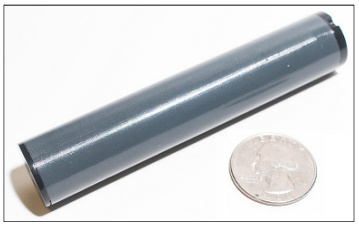

Fig. 5: The sensor package in a pressure barrel (Standard and "Extended-Battery-Life" version in ¾-in diameter)

The same sensors, electronics and battery can be packaged in a "hockey puck" shaped design for installation in a motor bit box and RSS bit box [28]. This design can also sample and record continuously at 800Hz or 1600Hz. **Fig. 6** shows the sensor in a "hockey puck" shaped package.

Fig. 6: Sensor in a "hockey puck" shaped package

Fig. 7 shows an example of the sensor installation in a bit

box and in an 8 ½-in drill bit.

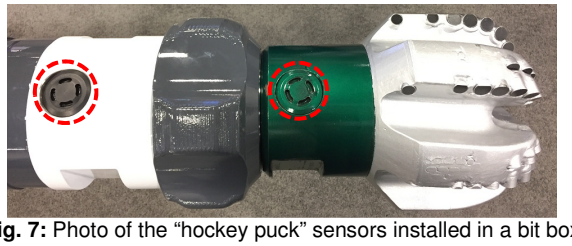

Fig. 7: Photo of the "hockey puck" sensors installed in a bit box and 8 ½-in drill bit shank

Field Example 1: 9 5/8-in RSS

A vertical 12 ¼-in. section was drilled with a motor-assist RSS in West Texas. The sensor package was embedded into the bit box of a 9 5/8-in push-the-bit RSS, which was run with a 9 5/8-in 7/8 4.0-stage motor (0.16 rev/gal). The length between the 12 ¼-in PDC bit and the top of the motor is approximately 58 ft (17.6 m).

Fig. 8a-8c show the FEA-simulated HFTO magnitudes and mode shapes for the first 3 modes. The normalized HFTO magnitudes are color-coded. The red area shows the highest HFTO magnitude, and the blue area shows the lowest HFTO magnitude. The first 3 HFTO frequencies simulated with the FEA software are 1) 19.6Hz, 2) 103.1Hz, and 3) 140.0Hz.

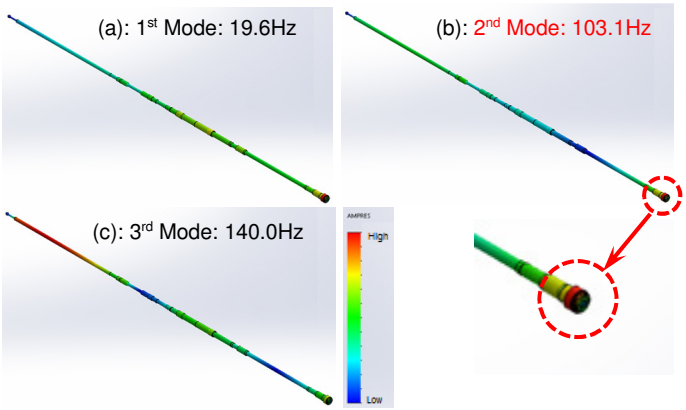

Fig. 8: FEA simulated HFTO magnitudes and mode shapes for the first 3 modes (Standard RSS)

As can be seen in Fig. 8a-8c, HFTO magnitude is higher (more red highlighted in a red circle) near the bit and near the surface of the structure.

The first 3 lateral natural frequencies from the FEA simulation are 1) 0.18Hz, 2) 1.7Hz, and 3) 5.9Hz. The lateral natural frequencies occur much lower than the torsional natural frequencies.

Using Eq. 1 with $G = 78.40\ GPa$ (shear modulus of the drillstring), $\rho = 7770\ Kg/m^3$ (density of the steel), $L = 17.6m$ (lower BHA length), and $n = 1$, the fundamental torsional oscillation frequency is estimated to be around 45.1Hz, which is more than twice as high as the FEA-simulated frequency. The discrepancy comes from the fact that the analytical solution assumes a uniform, circular-cross-section solid rod.

Fig. 9 shows the drilling dynamics data from the lower mandrel (bit box) of the 9 5/8-in RSS. The right-most spectrogram shows the frequency spectrum of the radial accelerometer. The frequency spectrogram consists of a series of Fourier analyses of the time-domain acceleration data [30]. The spectrograms show up to 400Hz as the sampling frequency is 800Hz, based on the Nyquist theorem [31].

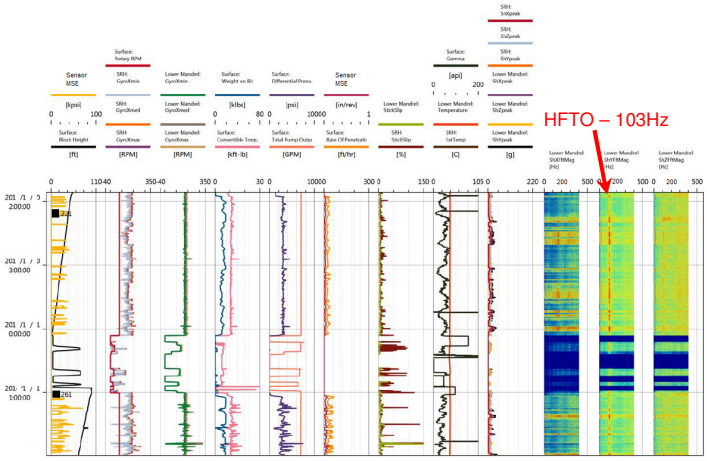

Fig. 9: Drilling dynamics data from the 800Hz-sampled embedded sensor

The second spectrogram from the right shows the frequency spectrum of the tangential accelerometer. The accelerometer axis convention is based on Bowler et al. (2014) [25] and Sugiura and Jones (2019) [12]. The dominant tangential acceleration frequency is approximately 103Hz, which is the second-order mode of the HFTO. The FEA-predicted HFTO frequency shows an excellent match with the downhole measured frequencies. The second-mode HFTO frequency calculated with the simple analytical model based on Eq. 1 is 135.4Hz, which is more than 31% off. We have learned that it is crucial to model the exact geometry and material type for the accuracy of the HFTO natural-frequency predictions.

The peak amplitude of the tangential acceleration due to the HFTO at the bit box is approximately 30-40g (60-80g peak-to-peak). The sensor offset distance is *3.3 in* (*0.084 meters*), thus the estimated peak angular acceleration is *3502-4670 rad/s*^{2}, based on **Eq. 2**.

$$\alpha = \frac{a_{tan}}{r} \quad \text{..... Eq. 2}$$

where α is the angular acceleration, a_{tan} is the tangential acceleration, and r is the offset radius, which is the distance between the tool center and the sensor position.

Sugiura and Jones (2019) have reported extreme HFTO cases, such as +200g peak (+400g peak-to-peak) [12]. So, the peak magnitude of 30-40g (60-80g peak-to-peak) at the bit can be considered as a "mild" HFTO case.

Field Example 2: 9 5/8-in "Short" RSS

A vertical and low-angle tangent 12 ¼-in sections were drilled with a motor-assist RSS in West Texas. The sensor package was embedded into the bit box of a 9 5/8-in push-the-bit RSS, which was run with a 9 5/8-in 7/8 4.0-stage motor (0.16 rev/gal). The length between the 12 ¼-in PDC bit and the top of the motor is approximately 56 ft (17.1 m). The length of the RSS mandrel was redesigned and shortened for the low-angle nudge rotary-steerable applications.

Fig. 10a-10c show the FEA simulated HFTO magnitudes and mode shapes for the first 3 modes. The normalized HFTO magnitudes are color-coded. The red area shows the highest HFTO magnitude, and the blue area shows the lowest HFTO magnitude. The FEA simulation has predicted the first 3 HFTO frequencies to be 1) 20.3Hz, 2) 105.9Hz, and 3) 143.2Hz. As expected, comparing against the longer RSS BHA used in the first field example, the HFTO frequencies are slightly higher from this RSS BHA.

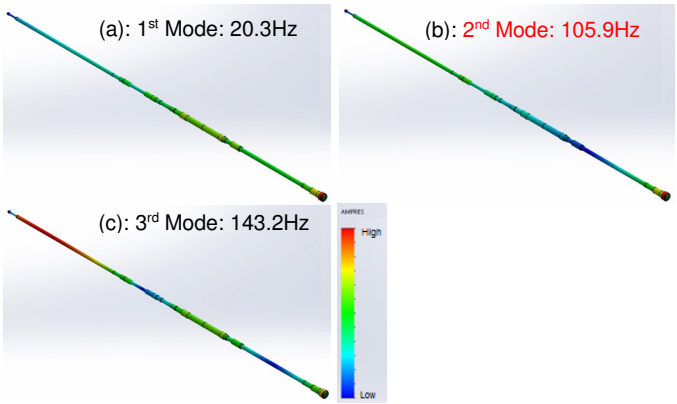

Fig. 10: FEA simulated HFTO magnitudes and mode shapes for the first 3 modes ("Short" RSS)

The first 3 lateral natural frequencies from the FEA simulation are 1) 0.19Hz, 2) 1.8Hz, and 3) 6.3Hz, which are much lower than the torsional natural frequencies.

Fig. 11 shows the drilling dynamics data from the bit box and the slow-rotating steering housing of the 9 5/8-in RSS. The right-most spectrogram shows the frequency spectrum of the bit-box radial accelerometer. The second spectrogram from the right shows the frequency spectrum of the bit-box tangential accelerometer. The dominant tangential acceleration frequency is approximately 106Hz, which is the second-order mode of the HFTO. The peak amplitude of the tangential acceleration is roughly 130g (260g peak-to-peak). The sensor offset distance is *3.3 in* (*0.084 meters*), thus the estimated peak angular acceleration is *15177 rad/s*^{2}, based on Eq. 2.

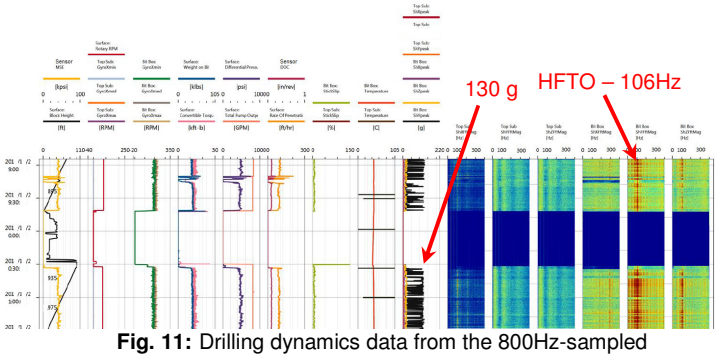

Fig. 11: Drilling dynamics data from the 800Hz-sampled embedded sensor (Short RSS)

The fourth spectrogram from the right shows the frequency spectrum of the radial accelerometer from the slow-rotating RSS housing, and the fifth spectrogram from the right shows the frequency spectrum of the tangential accelerometer from the slow-rotating RSS housing. No HFTO (106Hz) was observed from the tangential and radial accelerometers of the RSS housing. It is confirmed that the slow-rotating RSS housing de-couples the torsional dynamics coming from the drill bit and protects shock-sensitive sensors, electronics, electro-mechanical components and batteries from high-magnitude angular accelerations and tangential accelerations.

Field Example 3: 7 1/8-in RSS in Lateral

A lateral 8 ½-in section was drilled with a motor-assist RSS in West Texas. **Fig. 12** shows the high-frequency sensor package embedded into the bit box of a 7 1/8-in push-the-bit RSS, which was run with a 6 ¾-in 7/8 5.7-stage motor (0.24 rev/gal). An MWD tool was run below the motor. The length between the 8 ½-in PDC bit and the top of the motor is approximately 94 ft (28.7 m).

Fig. 12: 7 1/8-in RSS with embedded drilling dynamics sensors (in the blue circles) for drilling the 8 ½-in lateral section

Fig. 13a-13f show the FEA simulated HFTO magnitudes and mode shapes for the first 6 modes. The normalized HFTO magnitudes are color-coded.

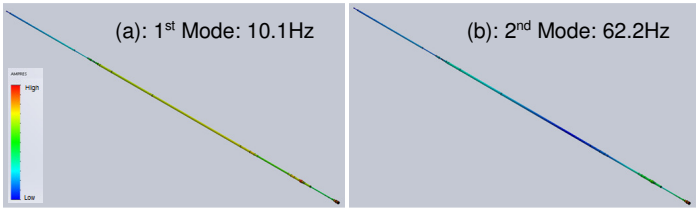

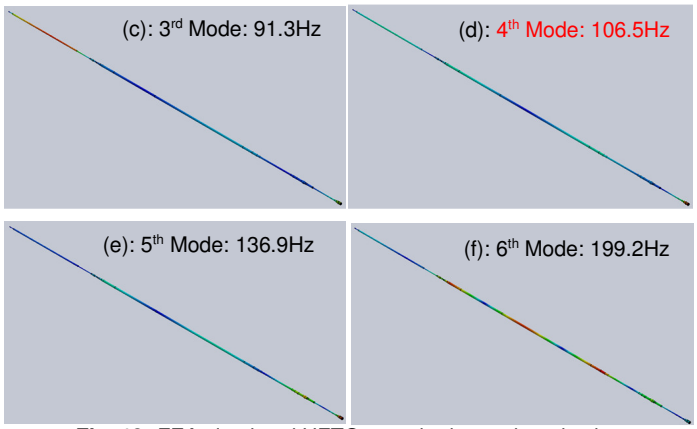

Fig. 13: FEA simulated HFTO magnitudes and mode shapes for the first 6 modes (7 1/8-in RSS)

The red area shows the highest HFTO magnitude, and the blue area shows the lowest HFTO magnitude. The first 6 HFTO frequencies predicted by the FEA simulation are 1) 10.1Hz, 2) 62.2Hz, 3) 91.3Hz, 4) 106.5Hz, 5) 136.9Hz, and 6) 199.2Hz. As expected, comparing against the 9 5/8-in RSS BHA used in the first and second field examples, the HFTO frequencies are much lower from this 7 1/8-in RSS BHA due to the longer distance between the bit and the top of the motor and smaller-diameter BHA.

Fig. 14 shows the drilling dynamics data from the bit box (or lower mandrel) of the 7 1/8-in RSS. The right-most spectrogram shows the frequency spectrum of the radial accelerometer. The second spectrogram from the right shows the frequency spectrum of the tangential accelerometer.

The dominant tangential acceleration frequency is approximately 107Hz, which is the fourth-order mode of the HFTO (based on Fig. 13d). The peak amplitude of the HFTO is roughly 130g (260g peak-to-peak) at the bit box, which can be seen from the violet curve in the fourth track from the right (Fig. 14). The sensor offset distance is *2.3 in* (*0.058 meters*), thus the estimated peak angular acceleration is *21980 rad/s*^{2}, based on Eq. 2. The peak angular acceleration of the 7 1/8-in RSS BHA (due to HFTO) is approximately 45% higher than that of the 9 5/8-in RSS BHA from Example 2 although the peak tangential acceleration values are similar, about 130g. This case illustrates the importance of taking the sensor offset distance (from the tool center) into consideration using Eq. 2.

Multiple HFTO Frequencies

In Fig. 14, the orange curve in the second track from the left shows the downhole-measured bit rotation speed (RPM) from the RSS bit box. The typical on-bottom, drilling bit rotation speed was about 200RPM. The blue curve in the fourth track from the left shows the surface-measured weight on bit (WOB) from the Electronic Drilling Recorder (EDR). The typical on-bottom, drilling WOB was about 30klbs. The pink curve in the same track shows the top-drive torque (typical on-bottom drilling values between 10-15kft-lbs). The violet curve in the fifth track from the left shows the surface total pump output in GPM (Gallons Per Minute). The typical on-bottom, drilling flow rate was about 600GPM. While the WOB was still very low (before the bit started engaging the formation), three distinct HFTO frequencies were observed, which is highlighted in a red dotted circle (top).

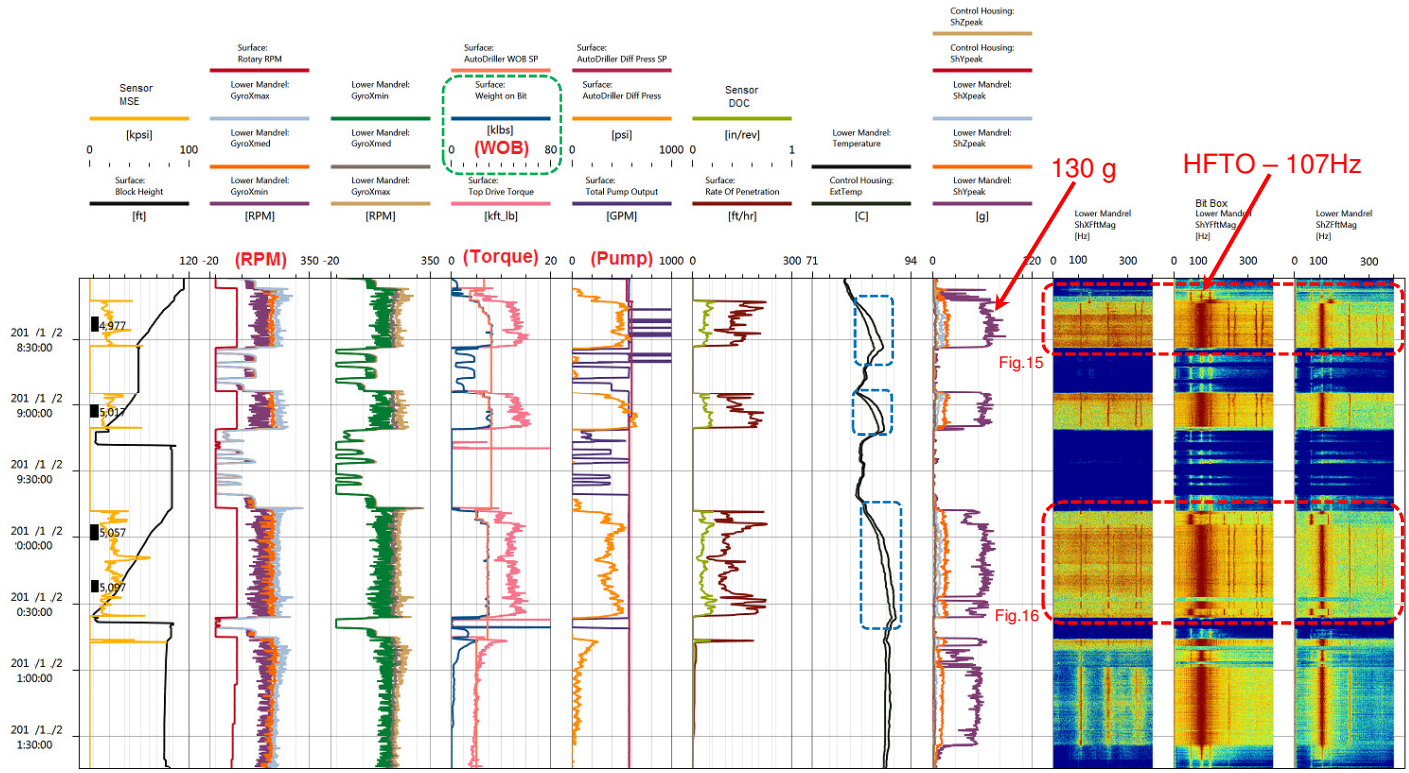

Fig. 14: Drilling dynamics data from the 800Hz-sampled embedded sensor (7 1/8-in RSS)

This section is zoomed in in **Fig. 15a-15c**, showing three oscillation frequencies in the spectrograms, which are (a) 63Hz, (b) 107Hz, and (c) 137Hz, respectively. These HFTO frequencies are the second mode, fourth mode, and fifth mode of the lower-BHA natural frequencies below the motor. These three HFTO frequencies were clearly observed while the WOB was ramping up from zero to 20klbs. It is observed that, for a short period of time when the WOB was approximately 20klbs, the dominant HFTO frequency became 137Hz (Fig. 15c), which is the 5th mode, based on Fig. 13e.

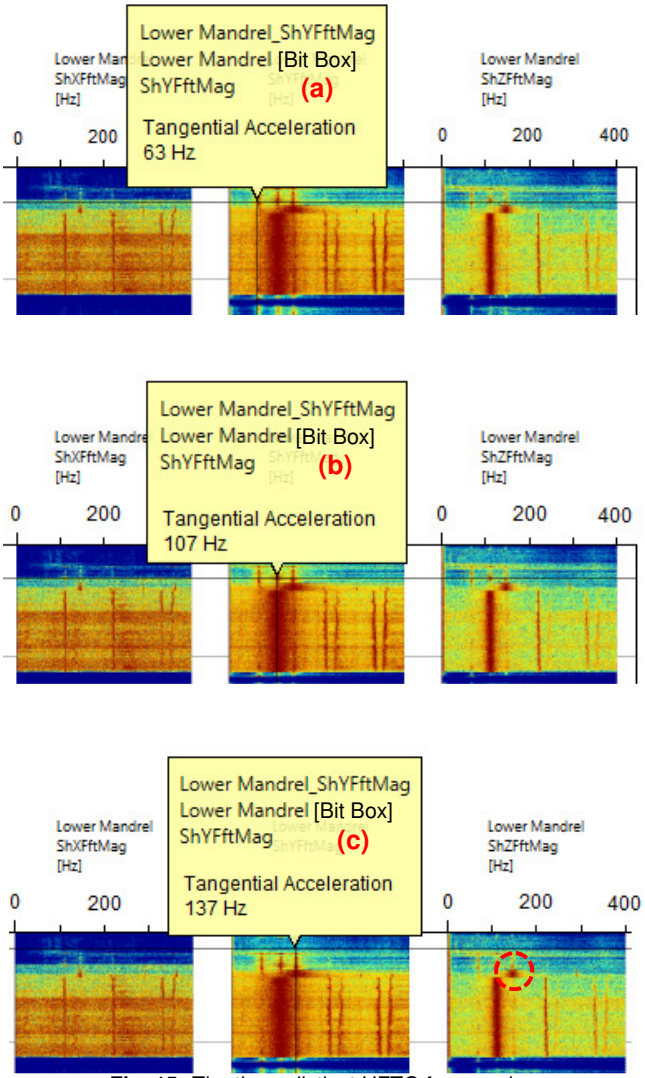

Fig. 15: The three distinct HFTO frequencies, (a) 63Hz, (b) 107Hz, and (c) 137Hz.

Dominant Frequency Switching

By looking at Fig. 15, there are three HFTO phases in the spectrograms: 1) low WOB (the blue curve in Fig. 14), below 10klbs, where three (relatively low-magnitude) HFTO frequencies are observed. There is no one dominant HFTO frequency, 2) WOB was ramping up from 10klbs to 20klbs, and the dominant HFTO frequency is 137Hz, which is the 5th mode, and 3) WOB is increasing to the nominal drilling weight from 20klbs to 30klbs and the dominant HFTO frequency shifted to 107Hz, which is the 4th mode.

Fig. 16 shows another example of the HFTO dominant frequency shifting, which can be observed from both tangential (middle) and radial (right) acceleration spectrograms.

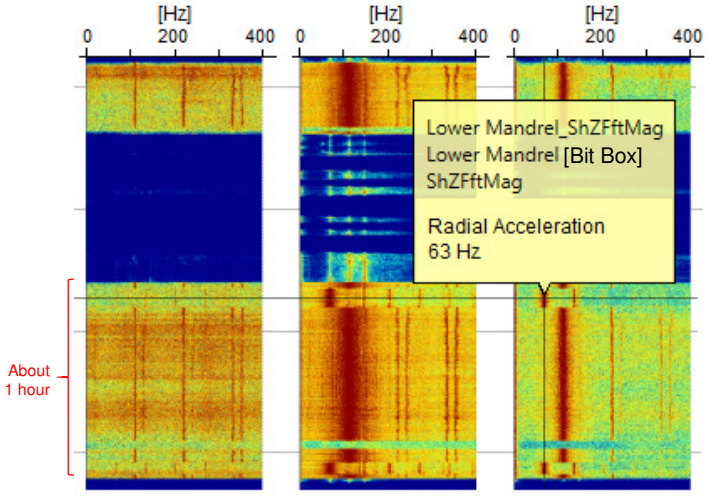

Fig. 16: Shifting of the dominant HFTO frequency from 63Hz to 107Hz and back to 63Hz.

The dominant frequency shifted from 63Hz to 107Hz and back to 63Hz. The lower dominant frequency of 63Hz (the 2nd mode shown in Fig. 13b) appeared at the beginning and end of the drill stand where the WOB was transitioning from 20klbs to 30klbs and 30klbs back to 20klbs. Another interesting observation from Fig. 16 is that the dominant HFTO frequency with the WOB range from slightly above zero to approximately 20klbs is 107Hz, for a very short period of time, about 1-2 minutes. Thus, the actual HFTO dominant-frequency shifting pattern in the one-hour interval is 1) 107Hz, 2) 63Hz, 3) 107Hz (majority of the time), 4) 63Hz and 5) 107Hz while drilling one stand.

It is confirmed that in this particular example, the lower HFTO dominant frequency of 63Hz is related to lower WOB (but not in the lowest WOB range) as the bit rotation speed and flow rate were both nearly constant at around 200RPM and 600GPM. The peak shock levels can be observed in the fourth track from the right in Fig. 14. The peak magnitude of the 63Hz HFTO (tangential accelerations) is slightly lower at approximately 75g peak (150g peak-to-peak) than that of the 107Hz HFTO, being around 130g peak (260g peak-to-peak).

Bit Temperature Rises

In Fig. 14, the fifth track from the right shows the sensor temperatures from the bit box and the slow-rotating housing. The bit (bit box) temperature rises are highlighted in blue dotted rectangles and are coincidental with the high level of the bit-box tangential accelerations (the fifth track from the right in violet).

Conclusions

Three HFTO field-test cases with dominant frequencies of 103-107Hz were shown to demonstrate that the peak tangential accelerations were up to 130g (or 260g peak-to-peak) with motor-assist 9 5/8-in and 7 1/8-in RSS BHA's. In the 9 5/8-in RSS BHA, the 2nd mode of HFTO (103Hz and 106Hz) was dominant. In the 7 1/8-in RSS BHA, the dominant frequency was 107Hz (the 4th mode) at least for the majority of the run.

Multiple HFTO dominant-frequency shifts were observed in the 7 1/8-in RSS BHA field data where the bit RPM and flow rate were essentially constant. It is concluded that WOB changes at the beginning and end of the stand affected the HFTO dominant-frequency shift. In the continuously recorded drilling dynamics data, a genesis of dominant frequency shift, namely from one dominant frequency (63Hz or 137Hz) to another (107Hz), was captured, giving a new insight of complex WOB, bit-rock interface and drilling systems interaction.

Acknowledgments

The authors would like to thank Turbo Drill Industries, Scout Downhole Inc., and Sanvean Technologies, LLC for their willingness to publish the data obtained with the motor-assist RSS and high-frequency drilling dynamics sensors and for permitting the publication of this work.

Special thanks to Chad Feddema and Rick Lee for their technical assistance and editorial work.

Nomenclature

BHA = Bottom-Hole Assembly
EDR = Electronic Drilling Recorder
GPM = Gallons Per Minute
HFTO = High-Frequency Torsional Oscillation
LFTO = Low-Frequency Torsional Oscillation
MWD = Measurement While Drilling
PDC = Polycrystalline Diamond Compact
ROP = Drilling Rate Of Penetration
RPM = Revolutions Per Minute
RSS = Rotary Steerable System
WOB = Weight On Bit

References

1. Lines, L. A., Stroud, D. R. H., & Coveney, V. A. (2013, March 5). Torsional Resonance - An Understanding Based on Field and Laboratory Tests with Latest Generation Point-the-Bit Rotary Steerable System. Society of Petroleum Engineers. doi:10.2118/163428-MS.
2. Lines, L. A., Mauldin, C. L., Hill, J. W., & Aiello, R. A. (2014, October 27). Advanced Drilling Dynamics Sensor Allows Real-Time Drilling Optimization, Damage Prevention and Condition Monitoring of RSS and LWD BHAs. Society of Petroleum Engineers. doi:10.2118/170586-MS.
3. Lines, L. (2016, October 1). Technology Update: A Holistic Approach to Controlling Torsional Dynamics in the Drillstring. Society of Petroleum Engineers. doi:10.2118/1016-0020-JPT.
4. Halsey, G. W., Kyllingstad, A., Aarrestad, T. V., & Lysne, D. (1986, January 1). Drillstring Torsional Vibrations: Comparison Between Theory and Experiment on a Full-Scale Research Drilling Rig. Society of Petroleum Engineers. doi:10.2118/15564-MS.
5. Kyllingstad, A., & Halsey, G. W. (1987, January 1). A Study of Slip-Stick Motion of the Bit. Society of Petroleum Engineers. doi:10.2118/16659-MS
6. Brett, J. F. (1992, September 1). The Genesis of Bit-Induced Torsional Drillstring Vibrations. Society of Petroleum Engineers. doi:10.2118/21943-PA.
7. Ledgerwood, L. W., Hoffmann, O. J., Jain, J. R., El Hakam, C., Herbig, C., & Spencer, R. (2010, January 1). Downhole Vibration Measurement, Monitoring, and Modeling Reveal Stick/Slip as a Primary Cause of PDC-Bit Damage in Today. Society of Petroleum Engineers. doi:10.2118/134488-MS.
8. Shen, Y., Zhang, Z., Zhao, J., Chen, W., Hamzah, M., Harmer, R., & Downton, G. (2017, October 9). The Origin and Mechanism of Severe Stick-Slip. Society of Petroleum Engineers. doi:10.2118/187457-MS.
9. Sun, Z. and Gu, Q. (2019, March 6). Mitigation of Multi-Frequency Stick/Slip. Society of Petroleum Engineers. doi:10.2118/194120-MS.
10. Ramakrishnan, G. (2019, March 6). Quenching of Self-Excited Vibrations in Multi Degree-of-Freedom Systems: Application to Stick-Slip Mitigation in Drilling. Society of Petroleum Engineers. doi:10.2118/194115-MS.
11. Zhang, Z., Shen, Y., Chen, W., Shi, J., Bonstaff, W., Tang, K., Smith, D.L., Alevalo, Y.I., & Jeffryes, B. (2017, October 9). Continuous High Frequency Measurement Improves Understanding of High Frequency Torsional Oscillation in North America Land Drilling. Society of Petroleum Engineers. doi:10.2118/187173-MS.
12. Sugiura, J. and Jones, S. (2019, March 6). A Drill Bit and Drilling Motor with Embedded High-Frequency (1600Hz) Drilling Dynamics Sensors Provide New Insights into Challenging Downhole Drilling Conditions. Society of Petroleum Engineers. doi:10.2118/194138-MS.
13. Dufeyte, M.-P., & Henneuse, H. (1991, January 1). Detection and Monitoring of the Slip-Stick Motion: Field Experiments. Society of Petroleum Engineers. doi:10.2118/21945-MS.
14. Alley, S. D., & Sutherland, G. B. (1991, January 1). The Use of Real-Time Downhole Shock Measurements to Improve BHA Component Reliability. Society of Petroleum Engineers. doi:10.2118/22537-MS.
15. Warren, T. M., & Oster, J. H. (1998, January 1). Torsional Resonance of Drill Collars with PDC Bits in Hard Rock. Society of Petroleum Engineers. doi:10.2118/49204-MS.
16. Belokobylskii S, Prokopov V K, "Friction-induced self-excited vibrations of drill rig with exponential drag law", International Applied Mechanics, vol. 18, no.12, pp. 1134-1138, 1982
17. Pastusek, P. E., Sullivan, E., & Harris, T. M. (2007, January 1). Development and Utilization of a Bit Based Data Acquisition System in Hard Rock PDC Applications. Society of Petroleum Engineers. doi:10.2118/105017-MS.
18. Oueslati, H., Jain, J. R., Reckmann, H., Ledgerwood, L. W., Pessier, R., & Chandrasekaran, S. (2013, September 30). New Insights into Drilling Dynamics through High-Frequency Vibration Measurement and Modeling. Society of Petroleum Engineers. doi:10.2118/166212-MS.
19. Jain, J. R., Oueslati, H., Hohl, A., Reckmann, H., Ledgerwood III, L. W., Tergeist, M., & Ostermeyer, G. P. (2014, March 4). High-Frequency Torsional Dynamics of Drilling Systems: An Analysis of the Bit-System Interaction. Society of Petroleum Engineers. doi:10.2118/167968-MS.
20. Oueslati, H., Hohl, A., Makkar, N., Schwefe, T., & Herbig, C. (2014, March 4). The Need for High Frequency Vibration

Measurement Along With Dynamics Modeling to Understand the Genesis of PDC Bit Damage. Society of Petroleum Engineers. doi:10.2118/167993-MS.

21. Hohl, A., Tergeist, M., Oueslati, H. et al. (2015, January 23). "Derivation and experimental validation of an analytical criterion for the identification of self-excited modes in drilling systems", Journal of Sound and Vibration, vol 342, pp 290-302.
22. Hohl, A., Tergeist, M., Oueslati, H., Herbig, C., Ichaoui, M., Ostermeyer, G.-P., & Reckmann, H. (2016, March 1). Prediction and Mitigation of Torsional Vibrations in Drilling Systems. Society of Petroleum Engineers. doi:10.2118/178874-MS.
23. Dennis, H., Mathäus, W., Christian, H., Andreas, H., & Hanno, R. (2017, November 13). High-Frequency Torsional Oscillation Laboratory Testing of an Entire Bottom Hole Assembly. Society of Petroleum Engineers. doi:10.2118/188370-MS.
24. Heisig, G., Sancho, J., & Macpherson, J. D. (1998, January 1). Downhole Diagnosis of Drilling Dynamics Data Provides New Level Drilling Process Control to Driller. Society of Petroleum Engineers. doi:10.2118/49206-MS.
25. Bowler, A. I., Logesparan, L., Sugiura, J., Jeffryes, B. P., Harmer, R. J., & Ignova, M. (2014, October 27). Continuous High-Frequency Measurements of the Drilling Process Provide New Insights into Drilling System Response and Transitions
26. Jones, S., Sugiura, J., Feddema, C., & Charter, M. (2018, March 6). A New Rotary-Steerable System Designed for Vertical and Nudge Applications in North America Pad Development Drilling. Society of Petroleum Engineers. doi:10.2118/189705-MS.
27. Jones, S., Sugiura, J., Rose, K., & Schnuriger, M. (2017, March 14). Drilling Dynamics Data Recorders Now Cost-Effective for Every Operator - Compact Embedded Sensors in Bit and BHA Capture Small Data to Make the Right Decisions Fast. Society of Petroleum Engineers. doi:10.2118/184738-MS.
28. Jones, S. and Sugiura, J., (2017, April 11). "Proven Mud Motor Technology Upgraded for the Digital Age – A Mud Motor with Embedded Sensors Provides Cost-Effective Drilling Dynamics Measurements at Bit Box and Stator Top Sub" presented at the 2017 AADE National Technical Conference and Exhibition, Houston, Texas, USA. AADE-17-NTCE-077.
29. Jones, S., Feddema, C., Castro, J., & Sugiura, J. (2016, March 1). Fully Mechanical Vertical Drilling System Delivers RSS Performance in Vertical Drilling Applications While Providing an Economical Alternative to Conventional Rotary Steerable Systems Set-Up for Vertical Hold Mode. Society of Petroleum Engineers. doi:10.2118/178788-MS.
30. Fourier, J.B.J. (1822), Théorie analytique de la chaleur (in French), Paris: Firmin Didot, père et fils.
31. Nyquist, H. 1928. Certain topics in telegraph transmission theory. Trans. AIEE. 47: 617-644.

Junichi Sugiura is the Vice President of Sanvean Technologies, Chartered Engineer (CEng), Chartered Petroleum Engineer, Chartered Energy Engineer, Fellow of the Institution of Engineering and Technology (FIET) and Fellow of the Energy Institute (FEI). He was formerly a Schlumberger Principal Engineer in UK. Sugiura's research interests include sensor technologies, artificial intelligence, data analytics, drilling dynamics/mechanics and directional drilling. He is the author/coauthor of 60 external publications and holds 48 US patents/pending patents in downhole technology. He holds a BS degree in Electrical Engineering Honors from the University of Texas at Austin.

Steve Jones is the President and CEO of Sanvean Technologies, which is the measurement and control-systems arm of Scout Downhole and Turbo Drill Industries. He has a BSc in Mechanical Engineering and an MSc in Mechanical and Offshore Engineering from the Robert Gordon University in Aberdeen, Scotland. He has published 20 technical papers on drilling technology and has 20 patents and pending patents worldwide. Steve has 24 years of experience in oil and gas drilling, specializing in directional drilling, rotary steerable, research-and-development, and product management.